

# Hydrothermal Preparation of Uniform Nanosize Rutile and Anatase Particles

Humin Cheng,\* Jiming Ma, Zhenguo Zhao, and Limin Qi

Department of Chemistry, Peking University, Beijing 100871, China

Received September 13, 1994. Revised Manuscript Received January 31, 1995<sup>®</sup>

Uniform nanosize rutile and anatase particles were prepared by a hydrothermal method using  $\text{TiCl}_4$  as starting material. The influences of various hydrothermal conditions on the formation, phase, morphology, and grain size of products were investigated and tentatively discussed from coordination chemistry. Increasing the acidity in reaction medium and the concentration of  $\text{TiCl}_4$  aqueous solution favored the formation of rutile type  $\text{TiO}_2$ . Raising the temperature ( $>200^\circ\text{C}$ ) can decrease the agglomeration among  $\text{TiO}_2$  grains. The mineralizers  $\text{SnCl}_4$  and  $\text{NaCl}$  reduce markedly the grain size and favor the formation of rutile type  $\text{TiO}_2$ . The mineralizer  $\text{NH}_4\text{Cl}$  will increase greatly agglomeration among grains. The optimum conditions for preparing rutile-type  $\text{TiO}_2$  were that  $[\text{TiCl}_4] > 0.5 \text{ mol dm}^{-3}$ ,  $220^\circ\text{C}$  for 2 h and using  $\text{SnCl}_4$  or  $\text{NaCl}$  as mineralizer. The average particle size of rutile  $\text{TiO}_2$  was 20 nm by 8 nm. The optimum conditions for preparing anatase type  $\text{TiO}_2$  were that  $\text{pH} > 7$ ,  $200^\circ\text{C}$  for 2 h. The average particle size of anatase  $\text{TiO}_2$  was ca. 10 nm. The Raman spectra of nanosize rutile and anatase were studied. With decreasing grain size of rutile, the all peaks broadened and their wavenumber decreased, while a new broad band near  $112 \text{ cm}^{-1}$  appeared gradually.

## Introduction

Titanium dioxide is commercially very important as a white pigment because of its maximum light scattering with virtually no absorption and because it is nontoxic, chemically inert, and a dielectric ceramic material for its higher dielectric constant. There are a lot of methods for preparing  $\text{TiO}_2$ .<sup>1–5</sup> Titanium dioxide is industrially produced generally by the so-called sulfate process and the so-called chloride process. In the former, the processing is very complicated. In the latter, the requirements for equipment and materials are very harsh because of high reaction temperature ( $>1400^\circ\text{C}$ ) and strong corrosiveness of  $\text{Cl}_2$  at high temperature. Comparing with other methods, the hydrothermal method has many advantages: (1) A crystalline product can be obtained directly at relatively lower reaction temperature (in general  $< 250^\circ\text{C}$ ). Hence the sintering process, which results in a transformation from the amorphous phase to the crystal phase, can be avoided. It favors a decrease in agglomeration between particles. (2) From a change in hydrothermal conditions (such as temperature, pH, reactant concentration and molar ratio, additive, etc.),

crystalline products with different composition, structure, and morphology could be formed. For example, perovskite-type (tabular), pyrochlore-type (starlike) and tetragonal body-centered type (acicular)  $\text{PbTiO}_3$ ,<sup>6,7</sup>  $\text{PbTi}_3\text{O}_7$ ,<sup>8</sup> and  $\text{PbO-TiO}_2$  solid solution ( $\text{PbTi}_x\text{O}_{1+2x}$ ,  $x = 0.8$ ) (tabular)<sup>9</sup> have been obtained under different hydrothermal conditions. In this work, rutile-type  $\text{TiO}_2$  (rodlike) and anatase-type  $\text{TiO}_2$  (granulose) have also been prepared under different hydrothermal conditions. (3) The purity of product prepared in appropriate conditions could be high owing to recrystallization in hydrothermal solution. (4) The equipment and processing required are simpler, and the control of reaction conditions is easier, etc. So the hydrothermal synthesis is a good method for the preparation of oxide ceramic fine powders. But research on the mechanism of hydrothermal reaction has seldom been reported. The main reason could be that the related thermodynamic data under hydrothermal conditions are much more scarce and usually limited to the Gibbs energies at 298.15 K. Lencka and Riman<sup>10</sup> made a beneficial attempt; they studied "Thermodynamic modeling of hydrothermal synthesis of ceramic powders" and obtained some interesting results. But on the other hand, they also indicated that the thermodynamic data used were most accurate at low and moderate temperatures

<sup>®</sup> Abstract published in *Advance ACS Abstracts*, March 1, 1995.

(1) Kamal Akhtar, M.; Xiong, Y.; Pratsinis, S. E. Synthesis of Titania Powder by Titanium Tetrachloride Oxidation in an Aerosol Flow Reactor. *Mater. Res. Soc. Symp. Proc.* **1992**, 249, 139–44.

(2) Tadafumi, A.; Katsuhito, K.; Kunio, A. Rapid and Continuous Hydrothermal Crystallization of Metal Oxide Particles in Supercritical Water. *J. Am. Ceram. Soc.* **1992**, 75, 1019–22.

(3) Jones, W. J.; Tooze, J. F. Eur. Pat. Appl., No. EP 0505022A1, 08.01.92.

(4) Kutty, T. R. N.; Vivekanandan, R.; Murugaraj, P. Precipitation of Rutile and Anatase ( $\text{TiO}_2$ ) Fine powders and their Conversion to  $\text{MTiO}_3$  ( $\text{M}=\text{Ba}, \text{Sr}, \text{Ca}$ ) by the Hydrothermal Method. *Mater. Chem. Phys.* **1988**, 19, 533–46.

(5) Hu, L.; Gu, Y.; Gu, J.; Han, J.; Chen, M. Preparation of Titania Ultrafine Particles via Hydrolysis of Titanium Alkoxides. I. Study of Hydrolysis and Particle Formation. *Huadong Huagong Xueyuan Xuebao* **1990**, 16, 260–65.

(6) Cheng, H.-M.; Ma, J.-M.; Zhao, Z.-G.; Zhang, H.-A.; Qiang, D.; Li, Y.; Yao, X. Hydrothermal Synthesis of Tabular Lead Titanate Fine Powders. In *Proceedings of C-MRS International' 90*; Han, Y., Ed.; Elsevier: Amsterdam, 1990; Vol. II, pp 509–14.

(7) Cheng, H.-M.; Ma, J.-M.; Zhao, Z.-G.; Qiang, D. Hydrothermal Synthesis of Acicular Lead Titanate Fine Powders. *J. Am. Ceram. Soc.* **1992**, 72, 1123–28.

(8) Kaneko, S.; Imoto, F. Reactions between  $\text{PbO}$  and  $\text{TiO}_2$  under Hydrothermal Conditions. *Bull. Chem. Soc. Jpn.* **1978**, 51, 1739.

(9) Cheng, H.-M.; Ma, J.-M.; Zhao, Z.-G. Hydrothermal Synthesis of  $\text{PbO-TiO}_2$  Solid Solution. *Chem. Mater.* **1994**, 6, 1033–40.

(10) Lencka, M. M.; Riman, R. E. Thermodynamic Modeling of Hydrothermal Synthesis of Ceramic Powders. *Chem. Mater.* **1993**, 5, 61.

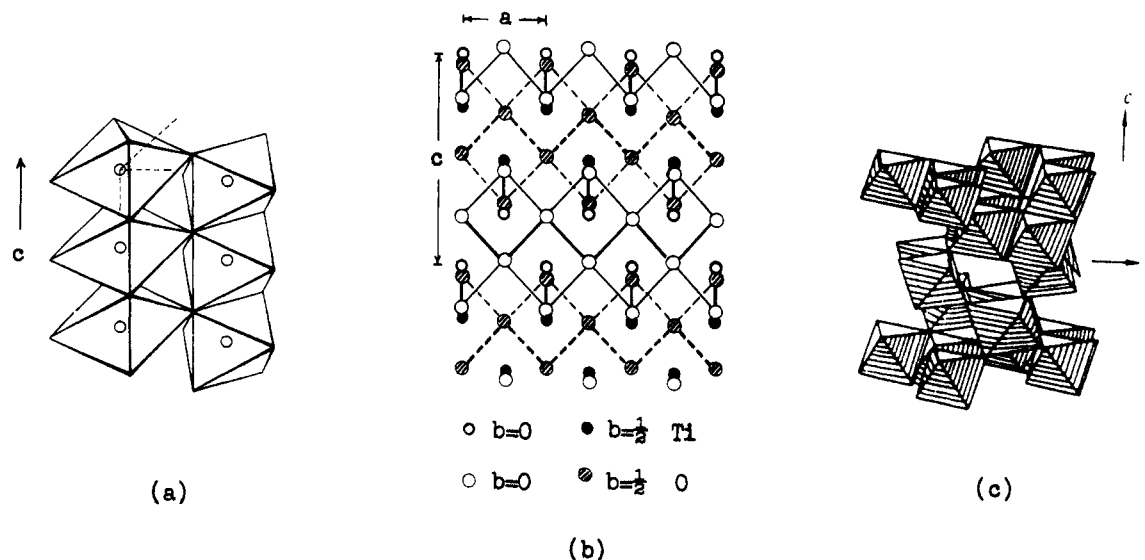


**Figure 1.** Modes of link among  $[\text{TiO}_6]$  octahedrons in (a) rutile, (b) anatase, the projection along the  $b$  axis (the thick line shows the edge-shared link), and (c) brookite.

and lose accuracy above ca. 473 K. So far the knowledge and experimental data for ions in hydrothermal systems, especially more complex ions such as  $\text{Ti}^{4+}$ ,  $\text{TiOH}^{3+}$ ,  $\text{Ti}(\text{OH})_2^{2+}$ ,  $\text{Ti}(\text{OH})_3^+$ , etc., are less well known. These caused difficulty for the research on the mechanisms of hydrothermal reaction.

Recently, ultrafine nanophase ceramics are attracting attention. Karch et al.<sup>11</sup> tested the low-temperature plastic deformation of nanocrystalline  $\text{TiO}_2$  and  $\text{CaF}_2$  ceramics and observed that conventionally brittle ceramics became ductile, permitting large (100%) plastic deformations at low temperature if a polycrystalline ceramic was generated with a crystal size of a few nanometers. This nanocrystalline  $\text{TiO}_2$  was obtained by oxidizing the small Ti crystals accumulated on the surface of the coldfinger. X-ray diffraction revealed this  $\text{TiO}_2$  to be pure rutile and its average crystal size of all specimens to be about 8 nm. The report about the hydrothermal preparation of nanosize  $\text{TiO}_2$  particles has been limited. The aim of the present work is to research the preparation of uniform nanosize rutile and anatase particles by the hydrothermal method and to make an attempt to discuss the influences of preparation conditions on the formation, morphology, phase, and particle size of the  $\text{TiO}_2$  products from coordination chemistry. In this paper, a grain is a small single crystal, and its size is determined by XRD. A particle is an identical one observed by TEM, which could be single crystal or polycrystal, and its size is measured with electromicrograph.

### Experimental Procedure

Titanium tetrachloride ( $\text{TiCl}_4$ ) was used as starting material. It was added slowly (ca. 1 mL  $\text{min}^{-1}$ ) into ice water (ca. 0 °C) under stirring to prepare a  $\text{TiCl}_4$  aqueous solution. The  $\text{TiCl}_4$  solution was filtered to remove insoluble species. The concentrations of three  $\text{TiCl}_4$  solutions determined by the gravimetric analysis were 1.40, 0.88, and 0.53 mol  $\text{dm}^{-3}$ , respectively. The pH in the medium was adjusted using KOH. The feedstock of 60 mL was charged into a 100 mL Teflon-lined stainless steel autoclave apparatus with an electromag-

netic stirrer (Peking University Instrument Factory). The hydrothermal preparations were conducted in the temperature range 85–220 °C for 1–4 h (heating rate 3 °C/ $\text{min}$ ). The influences of concentration of  $\text{TiCl}_4$  solution, pH in reaction medium, temperature, time, and mineralizer on the formation, phase, morphology, and particle size of  $\text{TiO}_2$  were examined. After the autoclave apparatus was cooled to room temperature in ca. 2 h, the product (suspension) was allowed to stand for 24 h and was filtered after removing the supernatant, washed with acetic acid–ammonium acetate buffer solution and alcohol in order to prevent peptization, and dried at 80 °C. The chemical agents used were all analytical reagent grade.

The prepared  $\text{TiO}_2$  powders were analyzed by X-ray diffraction (XRD) using Cu K $\alpha$  radiation at 40 kV and 100 mA and a graphite monochromator and by scanning at 2°  $2\theta$   $\text{min}^{-1}$  with a diffractometer (Model Dmax-2000, Rigaku Co., Tokyo, Japan) to determine the phase of the crystalline products. The morphology of products was observed using transmission electron microscopy (TEM, Model JEM-200 CX, JEOL Ltd., Tokyo, Japan). Differential thermal analysis (DTA) was conducted using DuPont 1090B thermal analysis systems (DuPont Co.). Raman spectra were detected with a Bruker FRA 106 FT-Raman accessory using a Nd:YAG laser ( $\lambda = 1064$  nm, 200 mW, Bruker Instrument Inc.). The surficial components of sample were analyzed with an electron spectrometer (Model VG ESCA LAB 5, VG Instrument Inc.) using Al K $\alpha$ ,  $HV = 50$  eV (FAT), 10 kV, 20 mA.

### Results and Discussions

The crystalline titanium dioxide has three crystalline forms: rutile, anatase, and brookite. Brookite and anatase are metastable and transform exothermally and irreversibly to the rutile over a range of temperatures but usually at 750 and 1000 °C, respectively.<sup>12</sup> The fundamental structure unit in three  $\text{TiO}_2$  crystals are all  $[\text{TiO}_6]$  octahedron, but their modes of arrangement and link are different. In rutile,  $[\text{TiO}_6]$  octahedrons link by sharing an edge along the  $c$  axis to form chains and then corner-shared bonding among chains leads to a three-dimensional framework.<sup>13</sup> In anatase, the formation of a three-dimensional framework is all with edge-shared bonding among  $[\text{TiO}_6]$  octahedrons.<sup>13</sup> The struc-

(12) Shannon, R. D.; Pask, J. A. Kinetics of the Anatase-Rutile Transformation. *J. Am. Ceram. Soc.* **1965**, *48*, 391–98.

(13) Wells, A. F. *Structural Inorganic Chemistry*, 4th ed.; Clarendon Press: Oxford, 1975; pp 143, 200.

(11) Karch, J.; Birringer, R.; Gleiter, H. Ceramics Ductile at Low Temperature. *Nature* **1987**, *330*, 556–58.

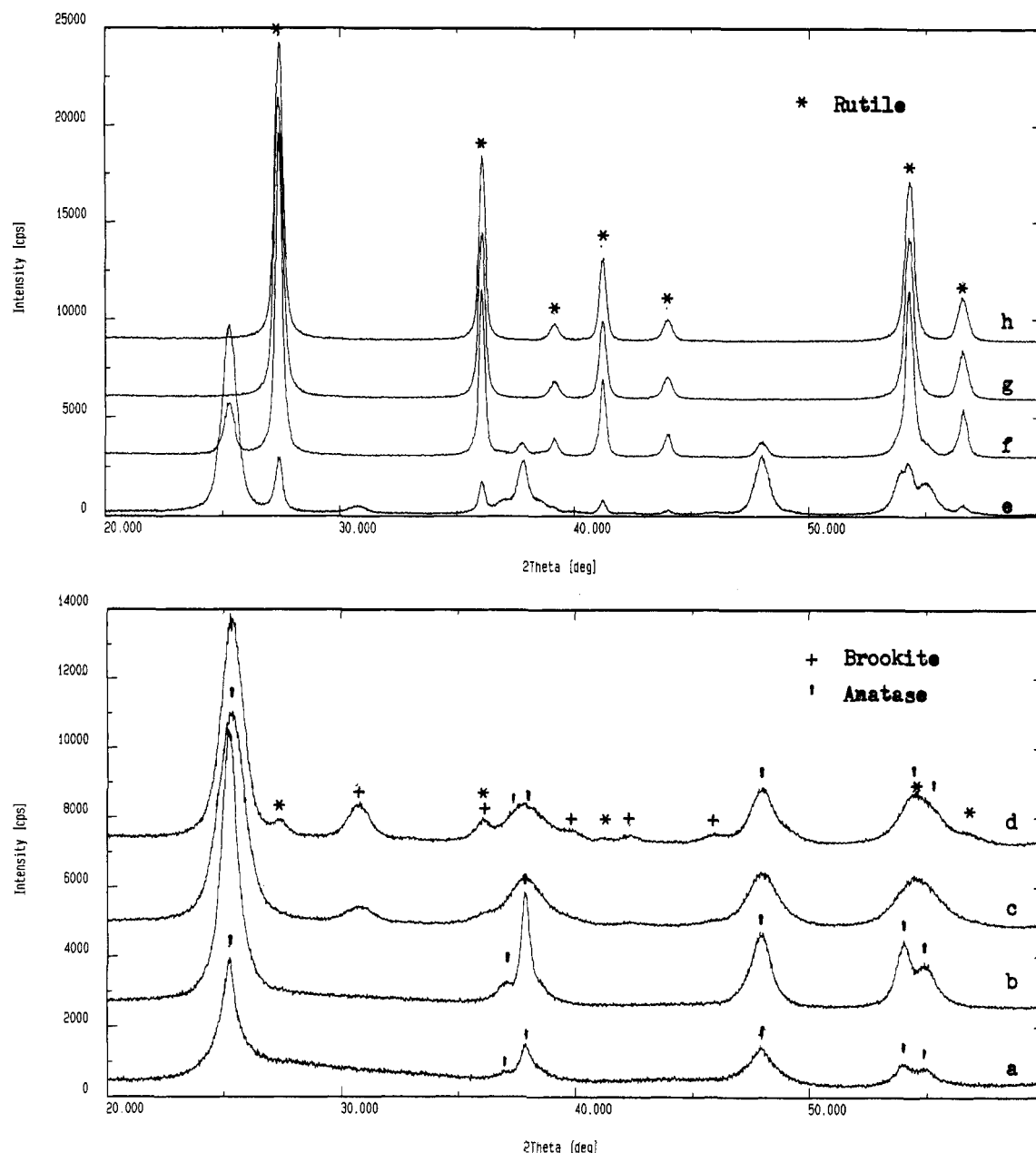


**Figure 2.** XRD patterns of the products prepared at different pH: (a–e) and  $[\text{TiCl}_4]$ : (f–h): (a) 8.2, (b) 7.1, (c) 3.4, (d) 1.0, (e) 0.0, (f)  $0.44 \text{ mol dm}^{-3}$ , (g)  $0.53 \text{ mol dm}^{-3}$ , (h)  $1.40 \text{ mol dm}^{-3}$ .

ture of brookite is slightly complicated and contains edge-shared and corner-shared bonding.<sup>14</sup> The modes of link among  $[\text{TiO}_6]$  octahedrons in three  $\text{TiO}_2$  crystals are shown in Figure 1.

Titanium dioxide prepared by the hydrothermal method can have different crystal structures and various morphologies, depending on the hydrothermal conditions. It could be concerned with the composition and structure of  $\text{Ti(IV)}$  complex ion in hydrothermal solution.

**(I) Influence of Hydrothermal Conditions. pH and Concentration in the Reaction Medium.** The pH in the reaction medium had a significant effect on the phase of  $\text{TiO}_2$  products. The feedstocks were prepared as follows: taking 30 mL of  $\text{TiCl}_4$  solution of  $0.88 \text{ mol}$

$\text{dm}^{-3}$ , using KOH solution to adjust the pH to the required value and concentration of titanium species in samples a–f (Figure 2) was kept to be  $0.44 \text{ mol dm}^{-3}$ . The reactions were conducted at  $220^\circ\text{C}$  for 2 h. The XRD patterns of the products prepared at different pH are given in Figure 2. The relevant TEM micrographs of products are shown in Figure 3. Figure 2 shows that high acidity is in favor of the formation of rutile phase. When the concentration of  $[\text{Ti}^{4+}]$  was  $0.44 \text{ mol dm}^{-3}$  (at this moment, the pH in the medium was negative and cannot be measured), the product was a mixture of rutile (majority) and anatase (minor) (Figure 2f) and had rodlike (rutile) and granulous (anatase) morphologies (Figure 3d). With increasing pH, the anatase phase in the products increased. As  $\text{pH} = 1.0$ , the product was mainly anatase and contained some brookite and a little rutile. When  $\text{pH} = 3.4$ , the rutile phase disappeared and the brookite phase in the product reduced. As  $\text{pH} = 7.1$ , the pure anatase phase with granulous morphol-

(14) Zhong, W.-Z.; Liu, G.-Z.; Shi, E.-W. et al. Growth Units and Formation Mechanism of the Crystals under Hydrothermal Conditions. *Sci. China, B*, 1994, 37, 1288.

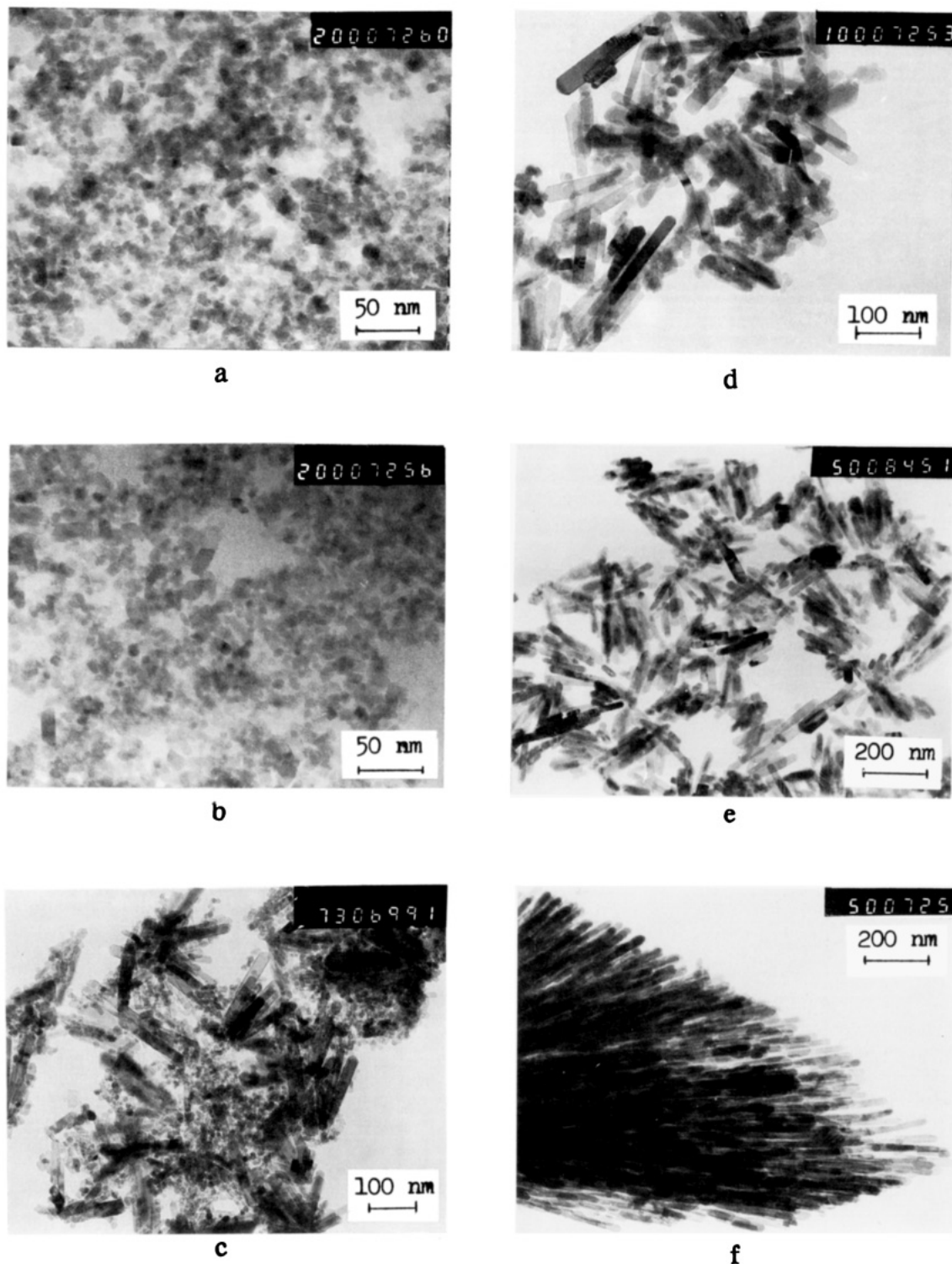


**Figure 3.** TEM micrographs of the products prepared at different pH: (a–c) and  $[\text{TiCl}_4]$ : (d–f): (a) 7.1, (b) 3.4, (c) 0.0, (d) 0.44 mol  $\text{dm}^{-3}$ , (e) 0.53 mol  $\text{dm}^{-3}$ , (f) 1.40 mol  $\text{dm}^{-3}$ .

ogy and grain size of ca. 10 nm was obtained (Figure 3a). If  $\text{pH} > 8$ , an amorphous phase began to appear, and when  $\text{pH} = 13$ , the product was quite amorphous. To obtain a pure rutile phase, it is necessary to further increase the acidity in the medium or the concentration of the  $\text{TiCl}_4$  solution.

The concentration of  $\text{TiCl}_4$  solution is increased while the acidity in reaction medium is also increased. The effect of concentration can be attributed mainly to the effect of acidity. Increasing the concentration of  $\text{TiCl}_4$  solution on one hand favors the formation of the rutile type  $\text{TiO}_2$  (Figure 2g and 2h) and, on the other hand,

will lead to agglomeration among  $\text{TiO}_2$  particles. For example, when the concentration of  $\text{TiCl}_4$  solution is 0.53 mol  $\text{dm}^{-3}$ , the agglomeration phenomenon is seldom observed and the particle size is quite uniform (about 100 nm by 10 nm) (Figure 3e), but as the concentration is increased to 1.40 mol  $\text{dm}^{-3}$ , rodlike rutile  $\text{TiO}_2$  grains agglomerated orientationally to form a broomlike aggregate, although every grain is still very small (Figure 3f).

From Figure 2, it can be seen that  $\text{TiO}_2$  formed at different acidity could have a different structure, which could be concerned with the coordination group of Ti-

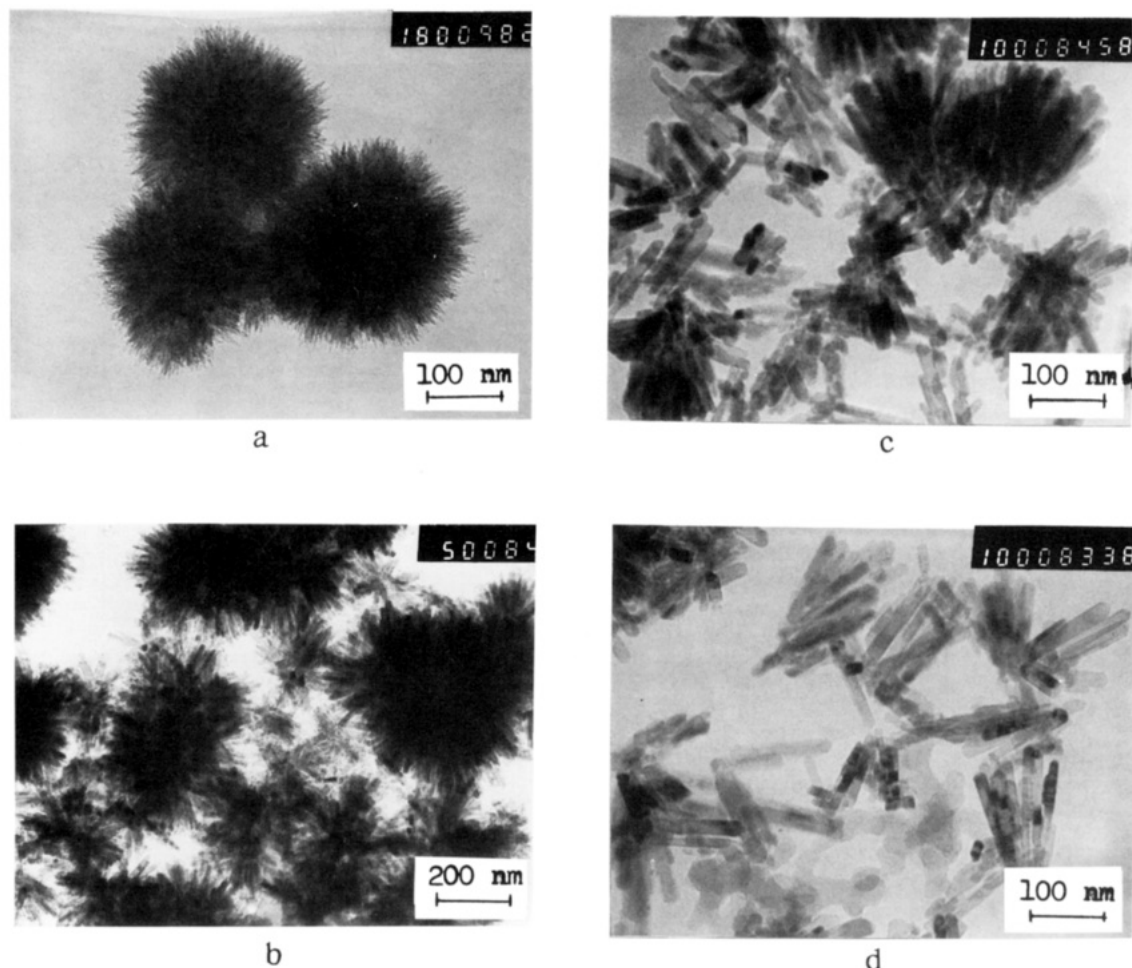


**Figure 4.** Effect of temperature on the agglomeration among grains: (a) 85 °C, (b) 180 °C, (c) 200 °C, (d) 220 °C ( $[\text{TiCl}_4]$  of 0.44 mol  $\text{dm}^{-3}$ , for 2 h).

(IV) complex ion. According to ligand field theory,  $\text{Ti(IV)} (3d^0)$  complex ions are all octahedrally coordinated in solution and crystal. The ligand field strength of OH group is larger than that of  $\text{Cl}^-$  ion. Nicholls<sup>15</sup> considered that in acids containing anions capable of coordinating to the titanium, the titanium(IV) was kept in solution as anionic complexes of type  $[\text{Ti}(\text{OH})\text{Cl}_5]^{2-}$  and  $[\text{TiCl}_6]^{2-}$ , because salts of this hexachlorotitanate(IV) anion can be precipitated from solutions of  $\text{TiCl}_4$  in saturated hydrochloric acid. Zhong et al.<sup>14</sup> investigated the electrophoretic experiment of a  $\text{BaTiO}_3$  solution ( $\text{Ba/Ti} = 1$ ) under hydrothermal conditions (250 °C, pH 7–8, 6 V, for 8 h) and found that brookite formed on the anode. It showed that titanium(IV) existed as an anionic coordinate polyhedron  $[\text{Ti}(\text{OH})_6]^{2-}$  in the above-mentioned solution. Hence the exact nature of titanium(IV) complexes depended on the acidity and ligand in solution. In the present work, it could be reasonable to assume that the  $\text{Ti(IV)}$  complex ion has the formula  $[\text{Ti}(\text{OH})_n\text{Cl}_m]^{2-}$  ( $\text{H}_2\text{O}$  could be a ligand too), where  $n + m = 6$ , and  $n$  and  $m$  are concerned with the acidity and concentration of  $\text{Cl}^-$  ion in feedstock, i.e., the higher the acidity and  $[\text{Cl}^-]$ , the bigger is  $m$ . The linking between  $[\text{TiO}_6]$  units is carried out by dehydration reactions (i.e., oxolation) between OH ligands in  $[\text{Ti}(\text{OH})_n\text{Cl}_m]^{2-}$  complex ions. When the acidity in feedstock is lower, the number of OH ligand in  $[\text{Ti}(\text{OH})_n\text{Cl}_m]^{2-}$  is more. In this

case, the probability of edge-shared bonding is larger, which could favor the formation of the anatase phase. As the acidity in feedstock is higher, the number of OH ligands in  $[\text{Ti}(\text{OH})_n\text{Cl}_m]^{2-}$  is less. Because the edge-shared bonding requires that two dehydration reactions between a pair of  $[\text{Ti}(\text{OH})_n\text{Cl}_m]^{2-}$  take place simultaneously, and therefore the edge-shared bonding could be suppressed and the corner-shared bonding may easily occur in higher acidity. Thus higher acidity and concentration of  $[\text{TiCl}_4]$  could be beneficial for the formation of rutile phase.

**Reaction Temperature and Time.** The temperature had a great effect on the grain size of the products and the agglomeration among grains. Lowering temperature will give rise to decreasing grain size and increasing agglomeration among grains. The concentrated aqueous  $\text{TiCl}_4$  solution ( $>0.5$  mol  $\text{dm}^{-3}$ ) was more steady at room temperature. As it was heated to about 85 °C, a white precipitate began to appear. After this, a vast amount of precipitate formed rapidly in ca. 10 min. The precipitate was filtered, washed, and dried at 80 °C. X-ray phase analysis and TEM observation indicated that the precipitate was a mixture of rutile (majority) and anatase (minor) with remarkable agglomeration although its average grain size was very small (ca. 5 nm from Debye–Scherrer formula). We further examined the effect of temperature in the range 180–220 °C. A group of samples with the major phase being rutile were used as examples. At 180 °C, the

(15) Nicholls, D. *Complexes and First-Row Transition Elements*; The Macmillan Press Ltd.: New York, 1974; Chapter 11.

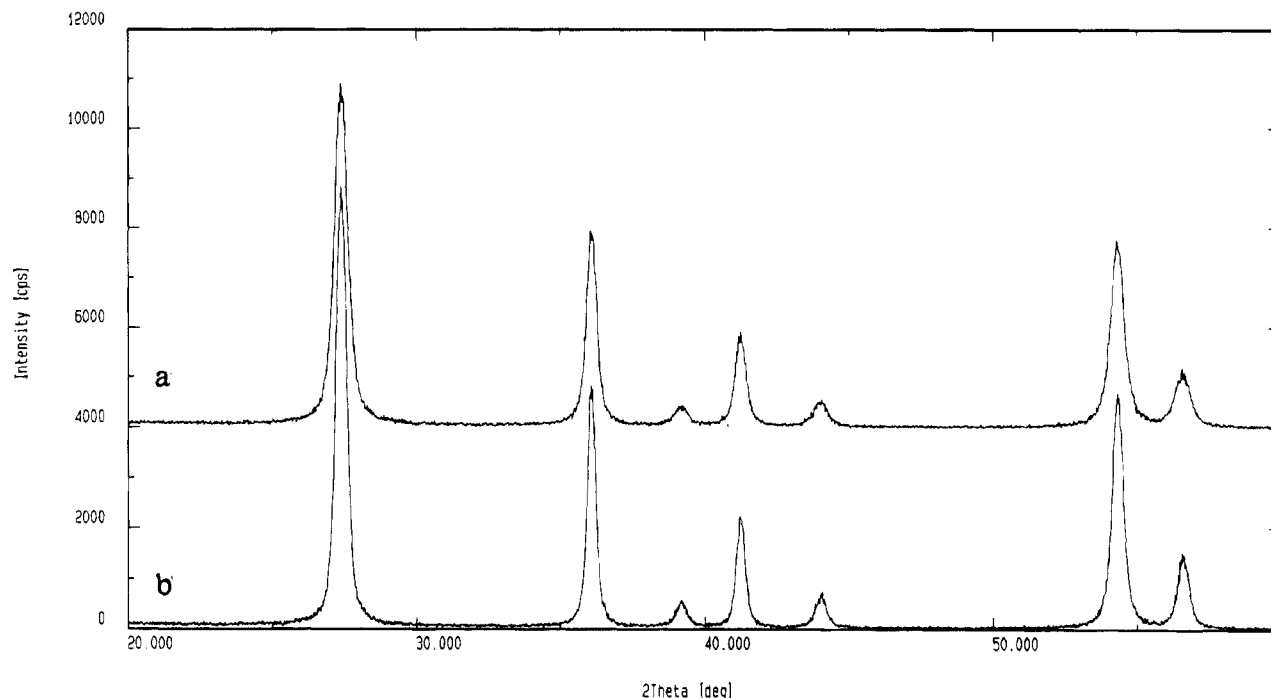


**Figure 5.** XRD patterns of the rutile samples prepared for different reaction time: (a) 1 h, (b) 2 h ( $[\text{TiCl}_4]$  of  $0.53 \text{ mol dm}^{-3}$ ,  $220^\circ\text{C}$ ).

**Table 1. Effect of Temperature on Grain Size<sup>a</sup>**

temp, $^\circ\text{C}$	HHB, deg	D, nm
180	1.00	8
200	0.76	10
220	0.59	14

<sup>a</sup> HHB, half-height breadth of (101) XRD peak for anatase. D, average grain size. Hydrothermal conditions:  $[\text{TiCl}_4]$  of  $0.27 \text{ mol dm}^{-3}$  for 2 h.

agglomeration phenomenon was still serious and did not disappear until the temperature rose to  $220^\circ\text{C}$ . The relevant TEM micrographs were shown in Figure 4. Decreasing temperature will give rise to the broadening of XRD peaks of the products, and it meant that the grain size of the products reduced. A group of samples with the major phase being anatase were used as examples. The effect of temperature on the grain size of the products was listed in Table 1. Prolonging the reaction time will make the grains grow, and the relevant XRD peaks were getting higher and sharper (Figure 5). It showed that the average grain size of products increased with prolonging reaction time. Their morphology essentially unchanged as Figure 3e.

The reasons for the agglomeration at lower temperature could be concerned with the large surface area of newly formed titanium dioxide particles. In strong acid medium, because the formation of  $\text{Ti(IV)}$  complex ions, the hydrolysis of titanium tetrachloride in water did not lead to the precipitation of much aqueous  $\text{TiO}_2$  at room temperature. Raising the temperature enhanced the hydrolysis of  $[\text{Ti}(\text{OH})_n\text{Cl}_{4-n}]^{2-}$  complex ions, i.e., the  $\text{Cl}^-$  ligand in it was substituted gradually by  $\text{OH}^-$  ligand, while the dehydration reactions between  $[\text{Ti}(\text{OH})_n\text{Cl}_{4-n}]^{2-}$  complex ions gradually took place to form crystalline  $\text{TiO}_2$ . This crystallite  $\text{TiO}_2$  easily formed an aggregate because of its large surface area. In the hydrothermal conditions, the recrystallization of small  $\text{TiO}_2$  particles enhanced to form regular  $\text{TiO}_2$  crystallite over  $200^\circ\text{C}$ ,

and the agglomeration phenomenon decreased relatively.

**Mineralizer.** We examined the effects of three mineralizers,  $\text{NH}_4\text{Cl}$ ,  $\text{NaCl}$ , and  $\text{SnCl}_4$ , on the titanium dioxide formed in hydrothermal reactions. Mineralizer solution (20 mL) was added to 50 mL of  $\text{TiCl}_4$  solution ( $0.44 \text{ mol dm}^{-3}$ ). The total volume of the feedstock was kept at 70 mL. The concentration of mineralizers  $\text{NH}_4\text{Cl}$ ,  $\text{NaCl}$ , and  $\text{SnCl}_4$  were 4, 4, and  $1 \text{ mol dm}^{-3}$ , respectively, to keep the total concentration of  $\text{Cl}^-$  in the reaction medium was constant. The other hydrothermal reaction conditions were temperature  $220^\circ\text{C}$  and reaction time 2 h. The results showed that these mineralizers had marked effects on the phase, morphology, and particle size of products. First, the three mineralizers were all in favor of the formation of rutile phase. The product was a mixture of rutile and anatase phase in the absence of mineralizer (Figure 2f) and a pure rutile phase in the presence of mineralizer. The XRD patterns of the relevant products were given in Figure 6. Second, the three mineralizers had different effects on the morphology and grain size of product. Ammonium chloride ( $\text{NH}_4\text{Cl}$ ) reduced grain size (XRD peaks broadened remarkably) but increased greatly agglomeration to form a hairy spheroid of particles. Sodium chloride ( $\text{NaCl}$ ) decreased particle size (from  $100\text{--}150 \text{ nm}$  by  $20 \text{ nm}$  to  $40 \text{ nm}$  by  $15 \text{ nm}$ ) and the agglomeration did not take place essentially. Tin tetrachloride ( $\text{SnCl}_4$ ) reduced markedly the particle size (to ca.  $20 \text{ nm}$  by  $8 \text{ nm}$ ), and the agglomeration phenomenon was not found, while the distribution of the particle size was uniform. Their electromicrographs were shown in Figure 7.

From Figure 6, it can be seen that the background was lower in the samples (b) and (c) but the background near  $2\theta = 26^\circ$ ,  $34^\circ$ , and  $51^\circ$  was higher in the sample (a). It indicated that very small crystallite  $\text{SnO}_2$  (tetragonal) was formed. ( $\text{SnO}_2$ : JCPDS-21-1250, the  $2\theta$



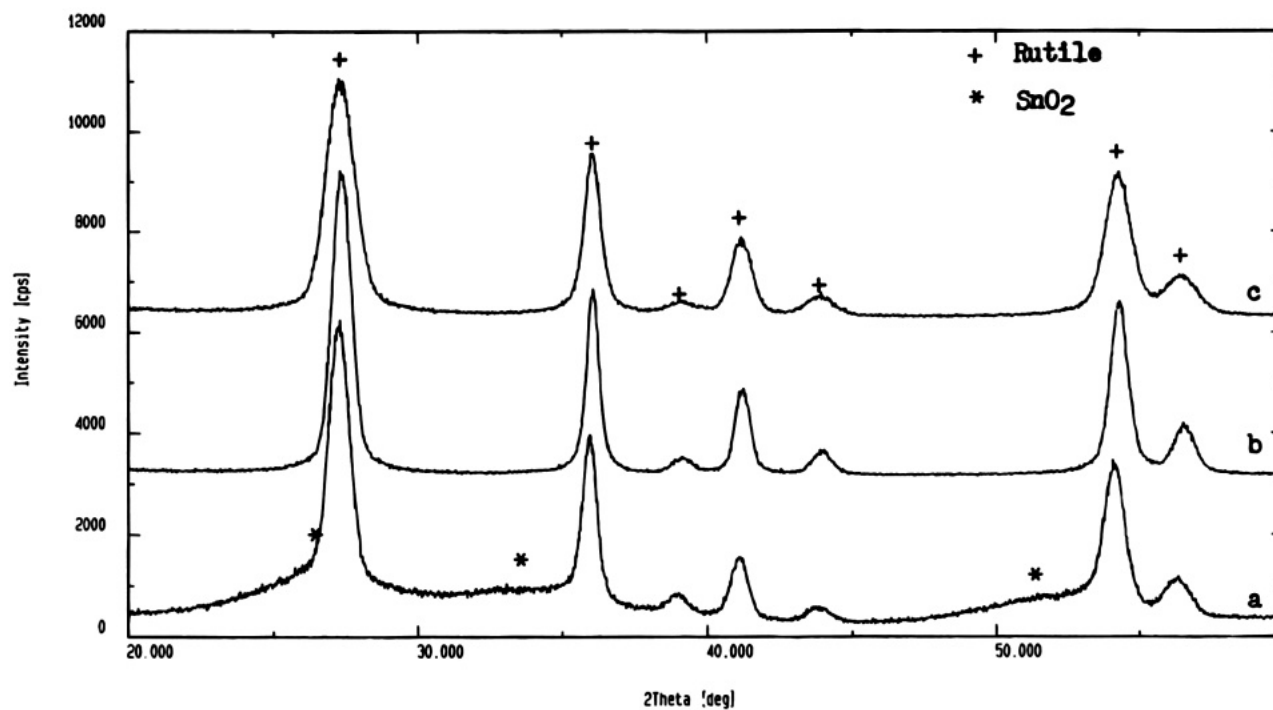
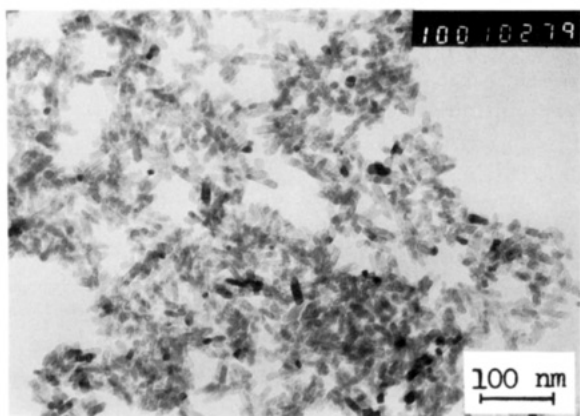
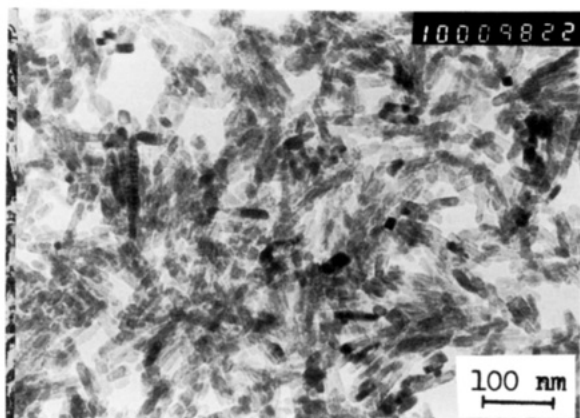
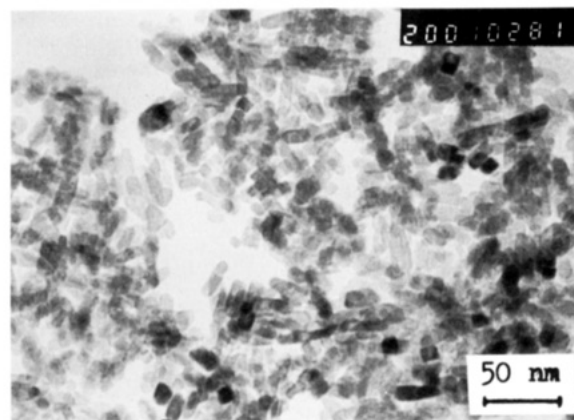


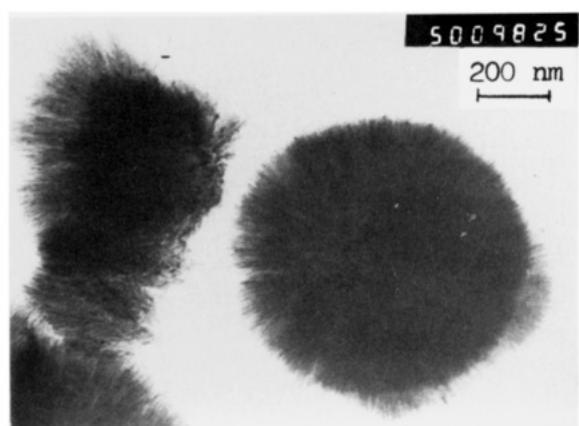
**Figure 6.** XRD patterns of products with different mineralizer: (a)  $\text{SnCl}_4$ , (b)  $\text{NaCl}$ , (c)  $\text{NH}_4\text{Cl}$  ( $[\text{TiCl}_4]$  of  $0.44 \text{ mol dm}^{-3}$ ,  $200^\circ\text{C}$  for 2 h).



a



b



c

**Figure 7.** TEM micrographs of the products with different mineralizer: (a)  $\text{SnCl}_4$ , (b)  $\text{NaCl}$ , (c)  $\text{NH}_4\text{Cl}$  ( $[\text{TiCl}_4]$  of  $0.44 \text{ mol dm}^{-3}$ ,  $200^\circ\text{C}$  for 2 h).

of its three strongest XRD peaks are at  $26.6^\circ$ ,  $33.9^\circ$ , and  $51.7^\circ$ , respectively). Because the tetragonal  $\text{SnO}_2$  has

the rutile-type structure, these crystallite  $\text{SnO}_2$  could grow on the surface of rutile  $\text{TiO}_2$  grains. Surfaceal

component analysis of the sample (6a) with the X-ray photoelectron spectrum (XPS) showed that before and after  $\text{Ar}^+$  ions etching (2 kV, 30  $\mu\text{A}$ , 1 min), the Sn/Ti atomic ratios on the surface of the sample were 1.30 and 0.51, respectively. It could be considered as evidence that  $\text{TiO}_2$  particles were coated by  $\text{SnO}_2$ .

Suyama et al.<sup>16</sup> and Akhtar et al.<sup>17</sup> investigated the effects of additives on the formation, phase, and particle size of  $\text{TiO}_2$  powders in vapor-phase synthesis. They considered that the additives could act as nucleating agents and changed the surface state of  $\text{TiO}_2$  particles to decrease the growth rate and inhibited the anatase-to-rutile transformation. The mechanism on effect of additives (or mineralizer) in hydrothermal reactions were seldom reported. Pyda et al.<sup>18</sup> studied the hydrothermal crystallization of zirconia and zirconia solid solutions. They found that sodium, potassium, and lithium hydroxides greatly influence both the morphology of the crystallites and their sizes and suggested that sticking of the elementary units in an ordered manner was the plausible mechanism of the elongated particle growth in the basic environments. Our experimental conditions were different from theirs. According to our investigations, the effects of additives in hydrothermal reactions could have two aspects: (1) The additive was adsorbed on the surface of crystallites. If the adsorption had selectivity to lead to a decrease in vertical growth rate of adsorbed crystal plane, which should result in the change of morphology of crystallite.<sup>6,7</sup> If the adsorption had not selectivity, the adsorbed additives on the surface may retard the deposition of the product component to decrease the growth rate, resulting in the reduction of the particle size.  $\text{SnO}_2$  has same crystal structure with  $\text{TiO}_2$  (rutile), therefore it was easily adsorbed on the surface of  $\text{TiO}_2$  to retard the growth of  $\text{TiO}_2$  particles and enhance new nucleation. The additive  $\text{SnCl}_4$  could play this role in hydrothermal synthesis of  $\text{TiO}_2$ . (2) The additive could affect the composition or coordination structure of the growth unit. The  $\text{OH}^-$  in  $\text{KOH}$  and the  $\text{Cl}^-$  in  $\text{NaCl}$  and  $\text{NH}_4\text{Cl}$  could act as this effect, while the larger  $\text{Na}^+$  and  $\text{NH}_4^+$  ions could be adsorbed on the negatively charged surface of  $\text{TiO}_2$  particles to prevent the growth of  $\text{TiO}_2$  particles. Thus the grain size of the product  $\text{TiO}_2$  was very small (XRD peaks broadened, Figure 6b,c) in the case of using  $\text{NaCl}$  and  $\text{NH}_4\text{Cl}$  as additives.

**(II) Differential Thermal Analysis (DTA).** The DTA curve of a typical nanosize rutile  $\text{TiO}_2$  sample ( $[\text{TiCl}_4]$  of 0.53 mol  $\text{dm}^{-3}$ , 220  $^\circ\text{C}$ , for 2 h) is shown in Figure 8. In the range of room temperature to 1000  $^\circ\text{C}$ , except for a small endothermic peak near 100  $^\circ\text{C}$  there are no considerable thermal effects. The endothermic peak near 100  $^\circ\text{C}$  is attributed to the desorption of the adsorption water on the surface of the sample. This result can be considered as collateral evidence to confirm this sample to be a pure rutile  $\text{TiO}_2$ .

**(III) Raman Spectrum.** The Raman spectrum of  $\text{TiO}_2$  has been studied extensively, but the investigation

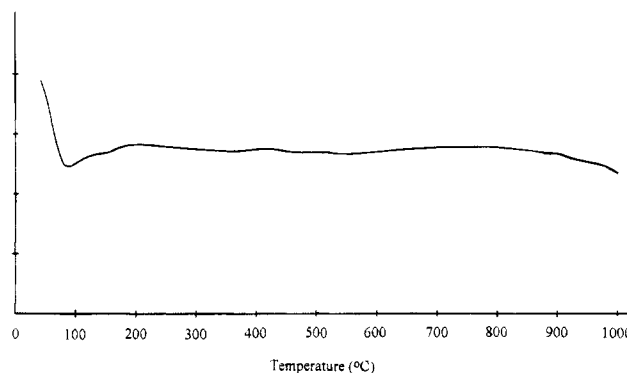


Figure 8. DTA curve of a nanocrystalline rutile  $\text{TiO}_2$ .

of the Raman spectrum of nanocrystalline  $\text{TiO}_2$  is limited. From previous work, in the Raman spectrum of rutile  $\text{TiO}_2$ , the band near 608  $\text{cm}^{-1}$  is identified as the  $\text{A}_{1g}$  mode, the band near 446  $\text{cm}^{-1}$  as the  $\text{E}_g$  mode, and the weak sharp band at 142  $\text{cm}^{-1}$  as the  $\text{B}_{1g}$  mode. The broad band near 240  $\text{cm}^{-1}$  is a second-order phonon as identified by Porto et al.<sup>19</sup> and confirmed by its disappearance in the 4.2 K spectrum.<sup>20</sup> Betsch et al.<sup>20</sup> researched the Raman spectra of stoichiometric and nonstoichiometric rutile crystals with prismatic morphology about 1 mm in cross section and 5–10 mm long in the range 4.2 K to room temperature. They discovered that the peak wavenumber of  $\text{A}_{1g}$  and  $\text{B}_{1g}$  modes in rutile crystal remained essentially constant with increasing temperature and changing stoichiometry but the  $\text{E}_g$  mode decreased by about 15  $\text{cm}^{-1}$  between 4.2 and 480 K in stoichiometric rutile and by about 6  $\text{cm}^{-1}$  between 80 and 300 K in nonstoichiometric rutile. They considered that the Raman line widths of rutile were an anomalous line broadening caused by a dynamic disorder phenomenon of the  $\text{TiO}_6$  octahedra. Melendres et al.<sup>21</sup> investigated the Raman spectroscopy of nanophase  $\text{TiO}_2$ . Their results seemed to rule out the influence of grain size on the line sharpness of the rutile phonons at 600 and 418  $\text{cm}^{-1}$  (here, the peak wavenumber of  $\text{A}_{1g}$  and  $\text{E}_g$  modes were different from that in refs 19 and 20 and our work) and considered that intragrain defects dominated the shaping of the spectral features.

We measured the Raman spectra of four  $\text{TiO}_2$  samples (rutile: 3, anatase: 1) with different grain sizes. Three rutiles are referred to as  $\text{R}_1$ ,  $\text{R}_2$ , and  $\text{R}_3$ , respectively and the anatase is referred to as  $\text{A}_1$ .  $\text{R}_1$ ,  $\text{R}_2$ , and  $\text{A}_1$  are prepared by the hydrothermal method and have grain sizes of 20 nm by 8 nm (Figure 7a), 100–150 nm by 20 nm (Figure 3e) and 10 nm by 10 nm (Figure 3a), respectively.  $\text{R}_1$  is the rutile  $\text{TiO}_2$  coated by  $\text{SnO}_2$ , but no other bands were observed besides the characteristic bands of rutile  $\text{TiO}_2$  in the Raman spectrum of  $\text{R}_1$ .  $\text{R}_3$  is a chemical agent in analytical grade and with grain size of ca. 200 nm. The Raman spectra of  $\text{TiO}_2$  samples at room temperature are shown in Figure 9. From Figure 9, it can be seen that the Raman spectrum of  $\text{R}_3$  sample coincided essentially with that of stoichiometric

(16) Suyama, Y.; Kato, A. Effect of Additives on the Formation of  $\text{TiO}_2$  Particles by Vapor Phase Reaction. *J. Am. Ceram. Soc.* **1985**, *68* (5), C-154.

(17) Akhtar, M. K.; Pratsinis, S. E. Dopants in Vapor-Phase Synthesis of Titania Powders. *J. Am. Ceram. Soc.* **1992**, *75*, 3408.

(18) Pyda, W.; Haberk, K.; Bucko, M. M. Hydrothermal Crystallization of Zirconia and Zirconia Solid Solution. *J. Am. Ceram. Soc.* **1991**, *74*, 2622–29.

(19) Porto, S. P. S.; Fleury, P. A.; Daman, T. C. Raman Spectra of  $\text{TiO}_2$ ,  $\text{MgF}_2$ ,  $\text{ZnF}_2$ ,  $\text{FeF}_2$  and  $\text{MnF}_2$ . *Phys. Rev.* **1967**, *154*, 522–26.

(20) Betsch, R. J.; Park, H. Lee; White, W. B. Raman Spectra of Stoichiometric and Defect Rutile. *Mater. Res. Bull.* **1991**, *26*, 613–22.

(21) Melendres, C. A.; Narayanasamy, A.; Maroni, V. A.; Siegel, R. W. Raman Spectroscopy of Nanophase  $\text{TiO}_2$ . *J. Mater. Res.* **1989**, *4*, 1246–50.



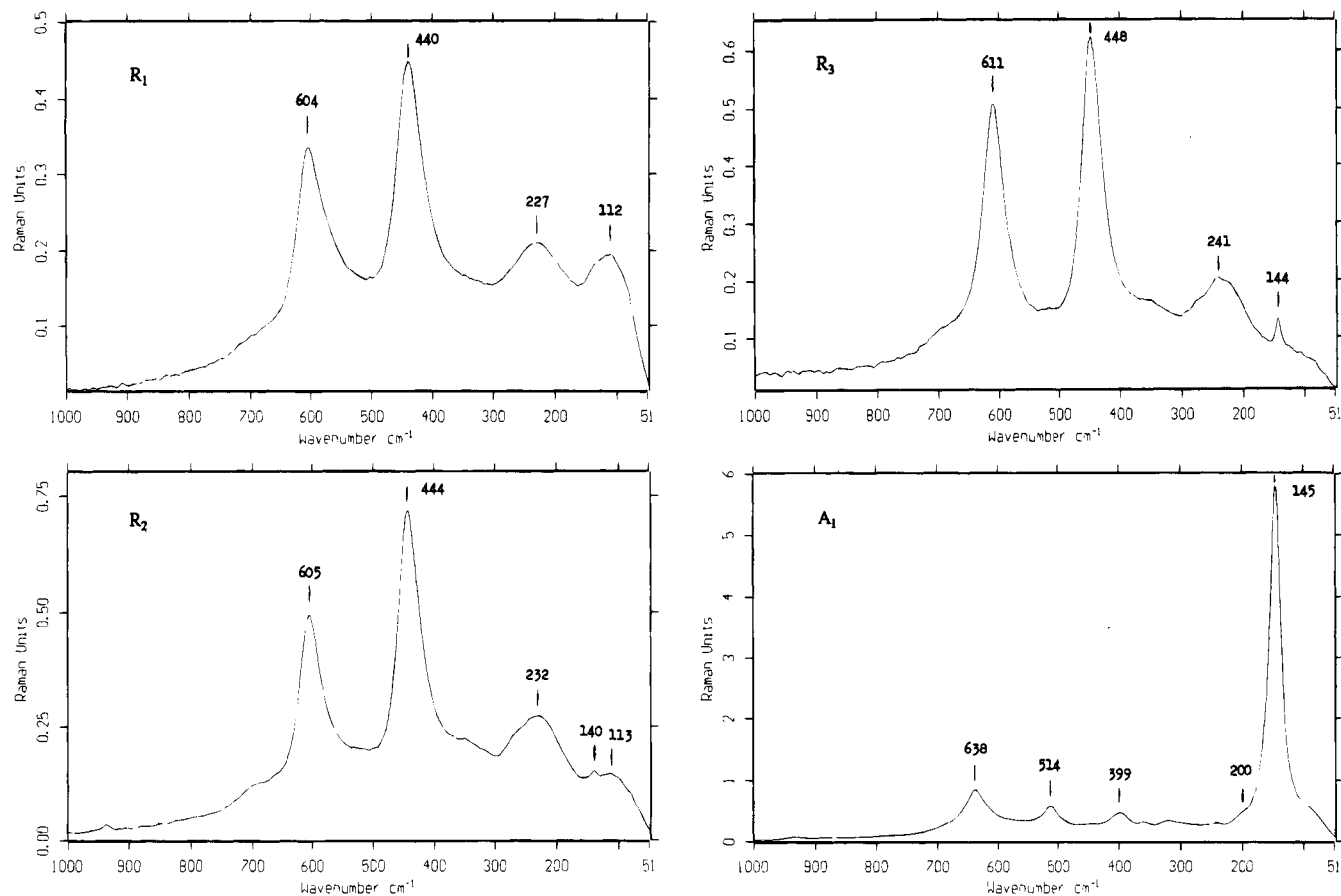


**Figure 9.** Raman spectra of several  $\text{TiO}_2$  samples:  $R_1$ , rutile, 20 nm by 8 nm;  $R_2$ , rutile, 100–150 nm by 20 nm;  $R_3$ , rutile, ca. 200 nm;  $A_1$ , anatase, ca. 10 nm.

rutile crystal at 280 °C in ref 20. With decreasing grain size from  $R_3$  to  $R_1$ , the wavenumber of all peaks decreased relevantly; in particular, the  $E_g$  mode decreased by about 8  $\text{cm}^{-1}$ , while a new broad band near 112  $\text{cm}^{-1}$  appeared gradually and the band near 144  $\text{cm}^{-1}$  could be covered. Besides, with decreasing grain size, the peak height to half-width ratio also lowered. The rutile  $\text{TiO}_2$  particles prepared by hydrothermal method have regular morphology and less intragrain defects because of the recrystallization of  $\text{TiO}_2$  particles in the reaction medium. Therefore, the above-mentioned results could be considered an effect of grain size for nanocrystalline rutile  $\text{TiO}_2$ . The Raman spectrum of  $A_1$  sample consisted essentially with the result for anatase powders reported by Pawlewicz,<sup>22</sup> but all the peaks in  $A_1$  became more broad.

### Conclusions

Uniform nanosize rutile and anatase particles have been prepared by a hydrothermal method using  $\text{TiCl}_4$  aqueous solution as starting material. The hydrothermal conditions have significant effects on the formation, phase component, morphology, and particle size of titania products. High acidity and concentration of  $\text{TiCl}_4$  solution are in favor of the formation of rutile

phase. Lowering temperature and increasing concentration could lead to agglomeration among grains. Mineralizers ( $\text{SnCl}_4$ ,  $\text{NaCl}$ ,  $\text{NH}_4\text{Cl}$ , etc.) are advantageous to forming rutile phase and decreasing grain size, but  $\text{NH}_4\text{Cl}$  will promote agglomeration among grains. Selecting appropriate hydrothermal conditions, uniform nanosize  $\text{TiO}_2$  (rutile or anatase) particles could be obtained. The effects of acidity and concentration in feedstock, temperature, and mineralizers on growth unit and crystal structure of products were tentatively discussed from coordination chemistry. The hydrothermal method is a good method for preparing uniform nanosize rutile and anatase particles.

The differences between the Raman spectra of nanosize and normal rutile  $\text{TiO}_2$  were mainly that peaks broadened, the peak wavenumber decreased, and a new band near 112  $\text{cm}^{-1}$  appeared in the former. It could be considered as an effect of grain size for nanosize rutile  $\text{TiO}_2$ .

**Acknowledgment.** The authors thank Mr. Ting Wang of Bruker Instrument Inc., Beijing, for help in determining the Raman spectra, Prof. Jiuxin Qian of Peking University for the DTA, and Prof. Hui Zhong Huang of Peking University for XPS. This work was supported by NAMCC and BZACAM.

(22) Pawlewicz, W. T.; Exarhos, G. J.; Conaway, W. E. Structural Characterization of  $\text{TiO}_2$  Optical Coatings by Raman Spectroscopy. *Appl. Opt.* **1983**, *22*, 1837–40.